On the Impact of Thermal Gradients across Fluxgate Sensors on In-situ Magnetic Field Measurements

K. Greene[1], C. T. Hansen[1], and D. M. Miles[1]

[1]Univeristy of Iowa, Department of Physics and Astronomy, Iowa City, IA, USA

Corresponding author: Kenton Greene (kenton-greene@uiowa.edu)

Key Points:

- Space based fluxgate measurements often observe calibration anomalies which are sometimes attributed to thermal gradients across the sensor
- A low-cost method for characterizing a fluxgate over changes in temperature and temperature gradient is presented
- Imposing large thermal gradients across the sensor did not have a measurable effect on instrumental sensitivity, offset, or noise.

Abstract

Fluxgate magnetometers are an important tool for measuring space plasmas. In-situ magnetic field investigations often involve measuring small perturbations of a large background field, so robust instrument calibration is critical to accurately resolving geophysical signals. Fluxgate instruments aboard recent space science missions have observed calibration anomalies that have been attributed to thermal gradients across the sensor. Here we present data from a laboratory experimental investigation of effects of thermal gradients on fluxgate calibration and performance. A purpose-built laboratory apparatus fixed two thermal reservoirs at either end of a racetrack fluxgate sensor. Varying the reservoir temperatures allowed us to vary the sensor temperature and impose thermal gradients as large as 50 °C across a racetrack fluxgate sensor. We find that changes in instrumental sensitivity, offset, and noise can be explained purely by changes in the average temperature of the sensor without a dependence on the difference in temperature across the sensor. We suggest that invoking concept of a static thermal gradient inducing thermoelectric currents within the fluxgate core or sensor may not be appropriate to explain changes in instrumental sensitivity, offset, and noise that have been observed on orbit.

Plain Language Summary

Fluxgate magnetometers are important tools for studying magnetic fields in space. However, when a fluxgate sensor is exposed to changing temperatures on-orbit, the baseline measurement can be unstable, making it harder to accurately measure small magnetic fields. Some fluxgates experience on-orbit instabilities that are related, not just to the average temperature of the sensor, but also to differences in temperature across the sensor. We use a laboratory testing method to explore the relationship of temperature differences across a sensor to changes in instability of the measurement. While we observe a strong relationship between changes in instability and the average temperature of the sensor, we do not observe a meaningful relationship between instability and differences in temperature across the sensor.

1 Introduction

Fluxgate magnetometers (Primdahl 1979) are an important tool for measuring space plasmas. However, they have long been known to have variations in calibration due to thermal effects (Trigg et al., 1971, Acuña et al., 1978, Miles et al., 2017). On magnetospheric and planetary science missions, variations in fluxgate calibration and performance are common on-orbit, especially during and after eclipse when the sensor temperature changes suddenly. Thermally linked variations have been observed on many recent missions such as Swarm (Tøffner-Clausen et al., 2016), Cluster (Alconcel et al., 2014), GOES-16 (Loto'aniu et al., 2019), CHAMP (Lühr et al., 2013), The Magnetospheric Multiscale Mission (Bromund et al., 2021); CRRES (McNeil 1993), BepiColombo (Baumjohann et al., 2020) GEO-KOMPSAT-2A (Magnes et al., 2020), e-POP/Swarm-Echo (Miles et al., 2019) and GRACE (Olsen 2021).

If these calibration anomalies are large enough, they can make it difficult to reliably resolve phenomena that are important to investigations of magnetospheric physics and planetary geology. For example, measurements of the small-scale structure (> 0.5 nT) of the earth magnetic field using Swarm and CHAMP (Olsen et al., 2017) can inform studies of the formation of geological structures such as plateaus (Qiu et al., 2017). Statistical studies of the morphology of the Earth's field-aligned current systems (i.e. Gjerloev et al., 2011; Lühr et al., 2015) rely on multipoint measurements to resolve the small spatiotemporal magnetic fluctuations

that are indicative of energy transport between the magnetosphere and ionosphere. Calibration anomalies can make it difficult to meaningfully compare these spatially separated measurements. On planetary missions, the absence of a well-determined model field against which the instrument can be reliably calibrated makes calibration stability even more critical. Variations in calibration as small as a few nT could make it difficult to reliably resolve small magnetic structures in the Martian crustal field that are important to understanding the geological history of mars (Connerney et al., 2001).

However, changes in sensor calibration are sometimes attributed, not only to changes in average sensor temperature, but also to thermal gradients (Bauer et al., 1999, Loto'aniu et al., 2019; Bromund et al., 2021, Magnes et al., 2020) imposed across the sensor. These thermal gradients can be imposed on-orbit by heating of the magnetometer by the sun on one side, and by cooling to space on the other side, as well as self-heating of the coils and sensors.

Despite being commonly invoked to explain calibration anomalies on-orbit, there is limited literature that documents and quantifies the observed effects of thermal gradients. The Magnetospheric Multiscale Magnetometers experience variations in the calibration offsets as large as 2 nT during eclipse that the authors could not explain by changes in average sensor temperature alone and were attributed to thermal gradients imposed across the sensor (Bromund et al., 2021). Brauer et al. (1999) found that the instrumental sensitivity of the CHAMP magnetometer changed as much as 150 ppm when a thermal gradient of about 1°C was applied across the sensor and noted the "importance of correcting for thermal gradients in determining the calibration coefficients vs temperature" (Brauer et al., 1999). The GOES-16 magnetometers observed anomalous variations in the calibration offsets of 5 nT that were attributed to "thermal gradients across each sensor". (Loto'aniu et al., 2019). The GK-2A magnetometer experienced diurnal "sensor offset oscillations" as large as 4 nT that were "triggered by large temperature gradients" (Magnes et al., 2020).

Bromund et al. (2021) and Schnurr et al. (2019) suggested that these on-orbit calibration anomalies could be due, in part, to thermoelectric currents in the fluxgate sensor or core induced by thermal gradients. Proposed mechanisms for this phenomenon include thermoelectric effects, such as the Seebeck effect (Jain et al., 2014; Hou et al., 2016), which could potentially introduce a small anomalous field in the fluxgate core or bobbin. A thermal-gradient-induced thermoelectric effect has been demonstrated to affect the on-orbit stability of other types of magnetic sensors such as the absolute scalar magnetometers on Swarm (Jager et al., 2016; Ferreira et al., 2019).

However, it is often difficult to ascertain from data obtained on orbit, whether these temperature dependant variations observed during eclipse are due to processes internal to the sensor, or to changes in magnetic stray field from the spacecraft. For example, the CHAMP calibration team found that small changes in calibration during eclipse are caused by currents flowing from the solar panels reversing to drain the battery (Lühr et al., 2013).

To make matters more complicated, the concept of a thermal gradient imposed across a fluxgate sensor is often difficult or impossible to directly observe on-orbit. Fluxgate sensors are often limited to a single temperature sensor that may or may not be in the same thermal regime as various parts of a fluxgate sensor assembly, so the spatial topology of the thermal gradient must be indirectly inferred, often using the rate of change in temperature as a proxy for thermal gradient (i.e., Brauer et al., 1999) or via thermal modelling (i.e., Bromund et al., 2021).

Therefore, is it unclear whether these variations are driven by sudden temporal variations in temperature (thermal shocks) or by the spatial distribution of temperature imposed statically across the sensor (thermal gradients). The Swarm Vector Magnetometer observed changes in sensitivity that were due not only to the scalar sensor temperature but were also strongly correlated with a time dependant change in sensitivity that depended on the angle relative to the sun. This was attributed to "the thermal capacitance of the sensor" (Tøffner-Caulsen et al., 2016) rather than thermal gradients.

In this paper, we investigate whether static thermal gradients imposed across a fluxgate sensor in a controlled laboratory conditions cause changes in instrumental sensitivity, offset, and noise that are independent from those changes caused by variations in average sensor temperature. Laboratory testing allows us to isolate and separate these variables in a way that is usually not possible on-orbit.

2 Experimental Method

To investigate the effects of thermal gradients on fluxgate performance, a purpose-made testing apparatus was assembled that allowed for direct measurement of fluxgate core sensitivity, offset, and noise.

2.1 The Device Under Test

The fluxgate under test is a simple racetrack core geometry sensor (Figure 1) purpose-built for this experiment that is manufactured using the process described in Miles et al 2022 where a 6-81 molybdenum-nickel permalloy is cold-rolled into 50 μm-thick foil. A milling machine is used to cut the foil into 6.45 mm-wide by 31.45 mm-long racetrack washers. The racetrack washers are placed in the furnace, heat-treated, and stacked into a Torlon bobbin (Figure 1a), and interleaved with insulating layers of Kapton of the same geometry.

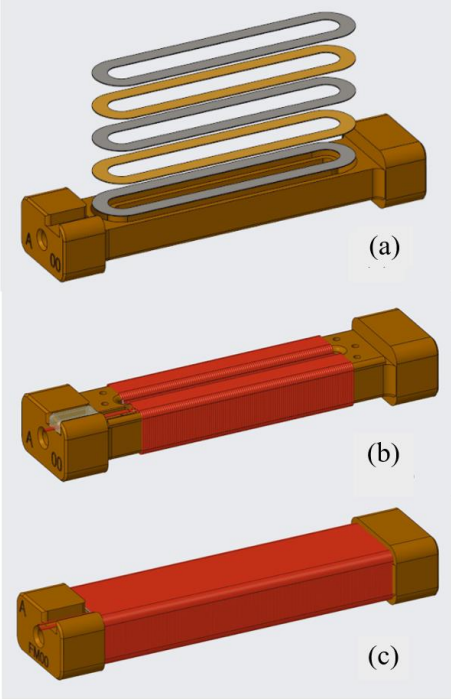

Figure 1. (a) The fluxgate device tested in the manuscript uses three layers of 6-81 Molybdenum permalloy washers which are interleaved with Kapton and placed inside a Torlon bobbin that supports (b) a quasi-toroidal winding of 32 AWG magnet wire serves as the drive winding (c) 34 AWG magnet wire wound in a solenoid directly on the bobbin acts as the sense winding.

The stacked foil washers remove the need to spot-weld, as is done in traditional spiral-wound sensors, avoiding the heat-affected area around the weld and its unpredictable magnetic properties (Miles et al., 2019). These racetrack cores were built for space applications and will be flight demonstrated in the new Tesseract high stability sensor (Greene et al., 2022) aboard the upcoming TRACERS SMEX missions as part of the MAGIC technology demonstration

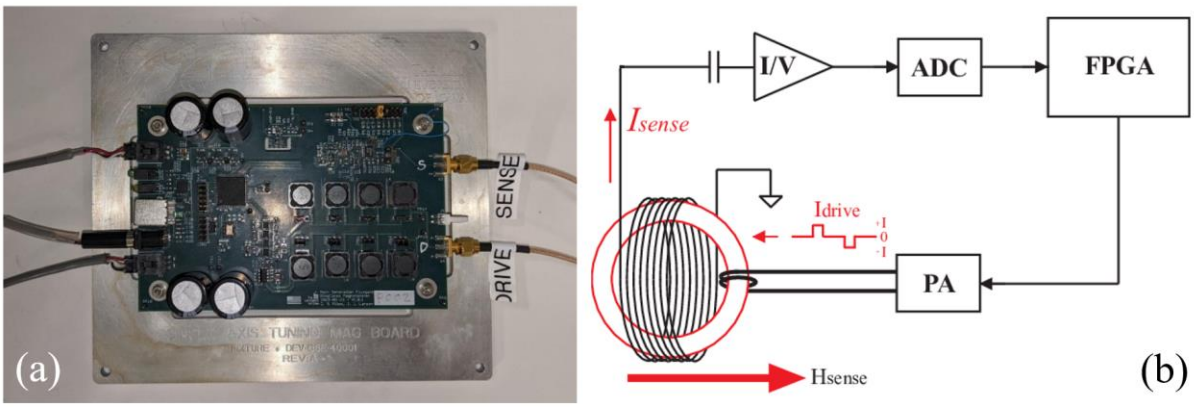

Figure 2. (a) An electronics board used in the testing described in the paper. (b) This board provided the drive current and filtered and digitized the output of the sense windings in an open loop.

An electronics board (Figure 2a) was used to drive all cores using ± 7.5 V at 5.0 kHz. To create the resonant drive current, the drive circuit used a series inductance of 11.1 mH and a

shunt capacitance of 2.4 uF. The fluxgate was tested in an open loop configuration (Figure 2b) to directly observe the intrinsic behaviour of the fluxgate sensor. A common shorted-coil pre-amplifier was used for the sense windings. A bandpass filter at the 2F frequency acted as the anti-aliasing filter and sensitivity for the fluxgate signal. The filtered signal was directly digitized at 10.0 ksps and averaged to 100 sps before being saved on the computer for analysis.

2.2 The Testing Apparatus

In order to test the effects of thermal gradients on this instrument's performance, a custom test apparatus was built. Both ends of the simplified fluxgate sensor were bolted to a purpose-built aluminium block using nylon screws. Water of different temperatures was pumped into the blocks through hoses so that they acted as thermal reservoirs (Figure 3a). Four Platinum RTDs were placed at different locations along the sensor to measure temperature and thermal gradient at different points along the sensor. The sensor and water blocks were placed inside a solenoid surrounded by a three-layer mumetal magnetic shield to fix the device in a controlled magnetic environment (Figure 3b). The inside edge of the solenoid is then lined with Polyurethane foam sheets to keep the solenoid and shield insulated.

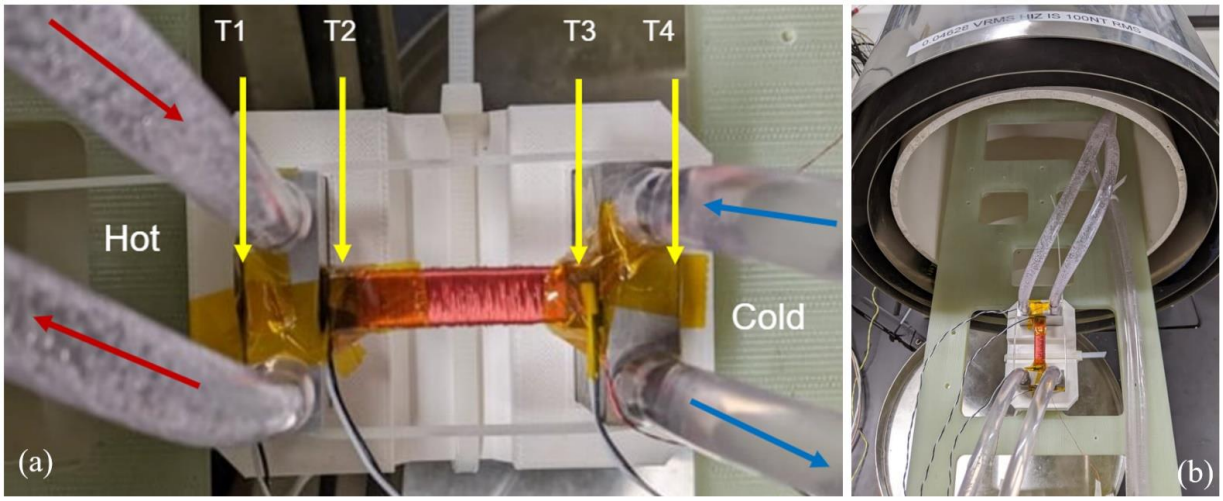

Figure 3 (a) A simplified fluxgate sensor bolted on each side to two aluminium blocks, that act as thermal reservoirs. Water of different temperatures was pumped into both blocks. The RTDs are labelled T1, T2, T3 and T4. T1 and T4 were secured to the hot and cold reservoirs respectively with Kapton. T2 and T3 were secured on either side of the Torlon bobbin (b) This apparatus was slid into solenoid surrounded by a three-layer mumetal magnetic shield to fix the apparatus a controlled magnetic environment.

The solenoid inside a three-layer mumetal magnetic shield was used to generate a constant amplitude 100 nT RMS, 1 Hz, AC magnetic field. The phasing of the direct digitization was adjusted to maximize the amplitude of the measured test signal. A linear scaling coefficient was then adjusted until the visualization software showed the test signal with the correct 100 nT rms amplitude to calibrate the transfer function of the complete open loop single-axis magnetometer.

The apparatus was arranged such that thermal gradients could imposed across the sensor (Figure 3a). In this configuration, the temperature of the water flowing through one block was

fixed at room temperature while water flowing through the second block was changed from 20 °C to 70 °C in increments of 5 degrees using a water heater. Figure 4a plots the temperature measured by each of the four RTDs over the course of one of these tests.

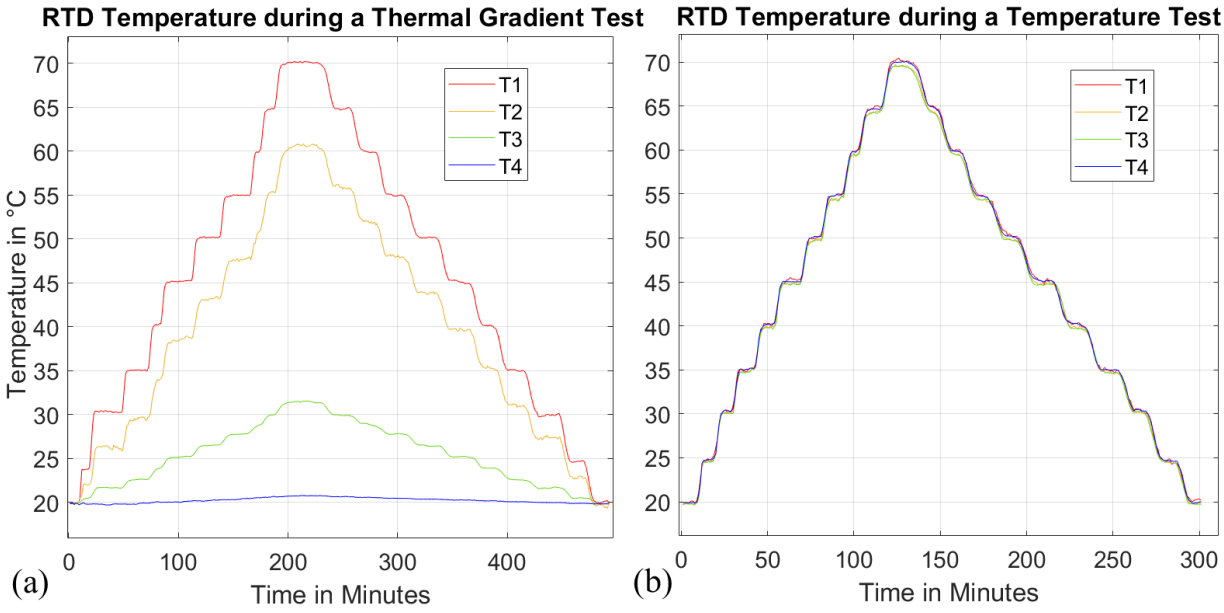

Figure 4 (a) The temperature measured by the four RTD sensors each at different points along the sensor during a thermal gradient test. The location of each of these sensors is shown in Figure 3a. Sensors T1 and T4 measure the temperature of the water blocks while T2 and T3 measure the temperature at two points along the sensor bobbin. (b) The temperature recorded by the RTD sensors during a temperature test is the same to within a few degrees C so there is little thermal gradient imposed across the sensor.

It is important to note that when the thermal gradient increases in this test, the average sensor temperature necessarily increases as well. To characterize effect of average sensor temperature, and to allow us to decouple it from the thermal gradient effects, a second test was run. The apparatus was rearranged so that each water block received water from the same source so that, while the average scalar temperature of the core varied, little to no gradient was imposed across the sensor (Figure 4b). The response of the fluxgate along with the voltage across the four RTD derived temperatures was digitized and recorded as the temperature of the water being pumped in the blocks was varied to change the overall temperature and the thermal gradient. For each test, the temperature was ramped up and back down to ensure that there are no asymmetric or hysteresis effects.

3 Results

The test described above was conducted three times to measure the dependence of the instrumental sensitivity, offset, and noise on the thermal gradient imposed across the core.

3.1 Sensitivity

This test was run to measure changes in sensitivity or scale factor of the fluxgate instrument with varying thermal gradients. In segments of the data where T2 and T3 are at the

same constant temperature for more than 5 minutes, a finite Fourier transform was used to calculate the amplitude of the applied sinusoidal test signal at 1 Hz. Figure 5a plots the amplitude of the measured field as a function of the 'average scalar temperature' which is just the average of the temperature measured by T1 and T4.

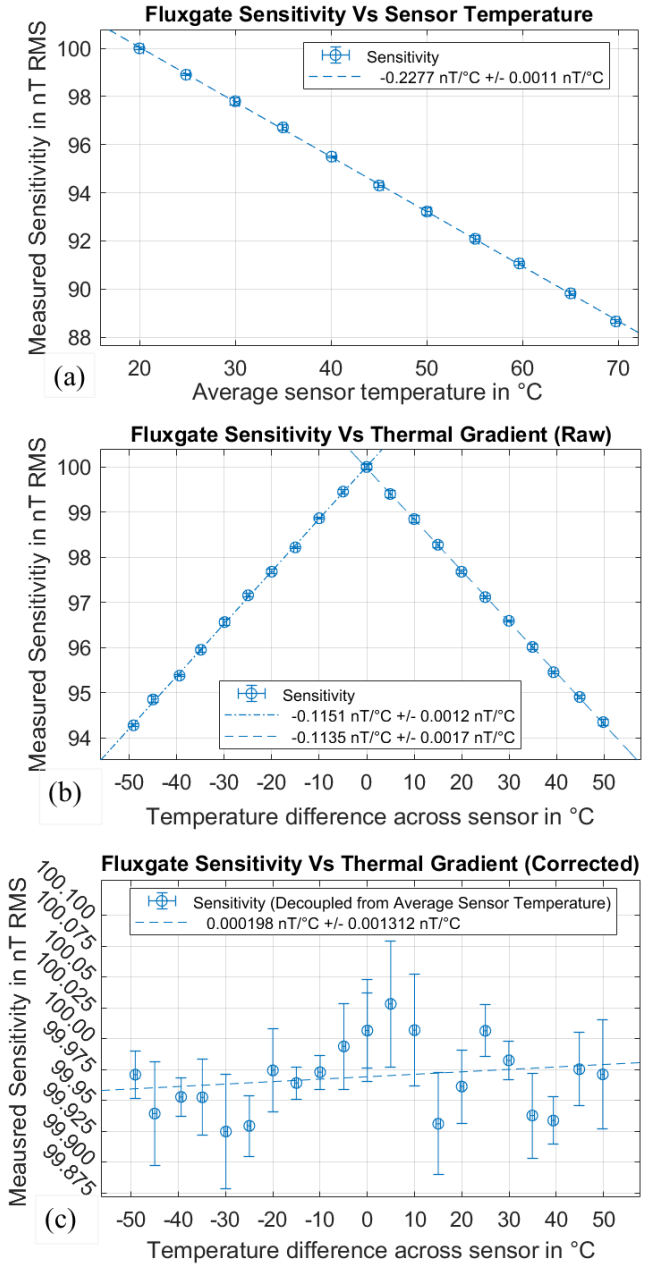

Figure 5 (a) The measured changes in sensitivity for sensor temperatures from 20 degrees to 70 degrees in intervals of 5 degrees. (b) The change in sensitivity is plotted against temperature difference between each end of the racetrack core. The slope of the sensitivity vs. temperature plot is almost exactly half the slope of sensitivity vs. thermal gradient plot. This suggests that the changes in sensitivity with thermal gradients can be explained entirely by the change in average temperature. (c) The fluxgate sensitivity over changes in thermal gradient when the change in average core temperature is accounted for and subtracted.

The configuration of the apparatus was then changed so that a temperature gradient was imposed over the core. The test started with both ends of the core fixed at 20 °C. One side was slowly ramped to 70 °C in increments of 5 °C while the other remained fixed at 20 °C. Figure 5b plots the measured change in sensitivity against the difference in temperature between each side of the fluxgate core. The same test was repeated in the same configuration except with the hot and cold-water supply hoses reversed to create a negative thermal gradient. Robust linear fits (MATLAB robustfit) were used to quantify the trend in each experiment.

The measured change in sensitivity over temperature (Figure 5a) is much larger than what would be expected if the instrument was configured in a temperature compensated closed feedback loop, which would be roughly equal the coefficient of thermal expansion of the torlon bobbin material as demonstrated by Acuña et al. (1978). Arranging the fluxgate in an open loop allows us to examine the underlying change in sensitivity with temperature; unsuppressed by feedback, which is much larger and is thought to be dominated by the temperature dependence of the apparent permeability of the fluxgate core material (Ripka 2008; Sebbes et al., 2010).

It is worth noting here that the sensitivity over thermal gradient data shown in Figure 5b does not account for the change in average scalar temperature defined as (T1+T4)/2 that necessarily occurs when one side was heated while the other side was held at room temperature. The raw sensitivity vs thermal gradient shown in Figure 5b is coupled with the average scalar temperature effect shown in Figure 5a. Figure 5c plots the change in sensitiviy over thermal gradient when the contribution of the average sensor temperature (Figure 5a) has been accounted for by subtracting the sensitivity vs temperature trend fit from 5a. A robust linear fit to the corrected data in Figure 5c shows that the sensitivity does not change by more than 0.0131 nT RMS for temperature differences across the length of the core ranging from -50 °C to 50 °C with confidence intervals of 95%.

3.2 Instrumental Offsets

The test was repeated with the applied sinusoidal field disabled so that only the DC background magnetic field in the shield was being measured. To measure the instrumental offsets, one hundred seconds of quite time data was recorded for at each temperature and thermal gradient. Then the custom-made fixture that holds the temperature blocks and the core (Figure 3a) was flipped 180 degrees, and another 5 minutes of data was taken. A channel machined on the bottom of the fixture allowed it to be fastened and aligned with the sliding plate 180 degrees from the original position. The offset at each temperature and gradient was calculated by the difference of the field measured when the apparatus is aligned with the shield, and the measured field when the apparatus is flipped 180 degrees. The uncertainties in the offset measurement estimated from the uncertainty of the aligment to the solonoid which was ussually around 1 degree.

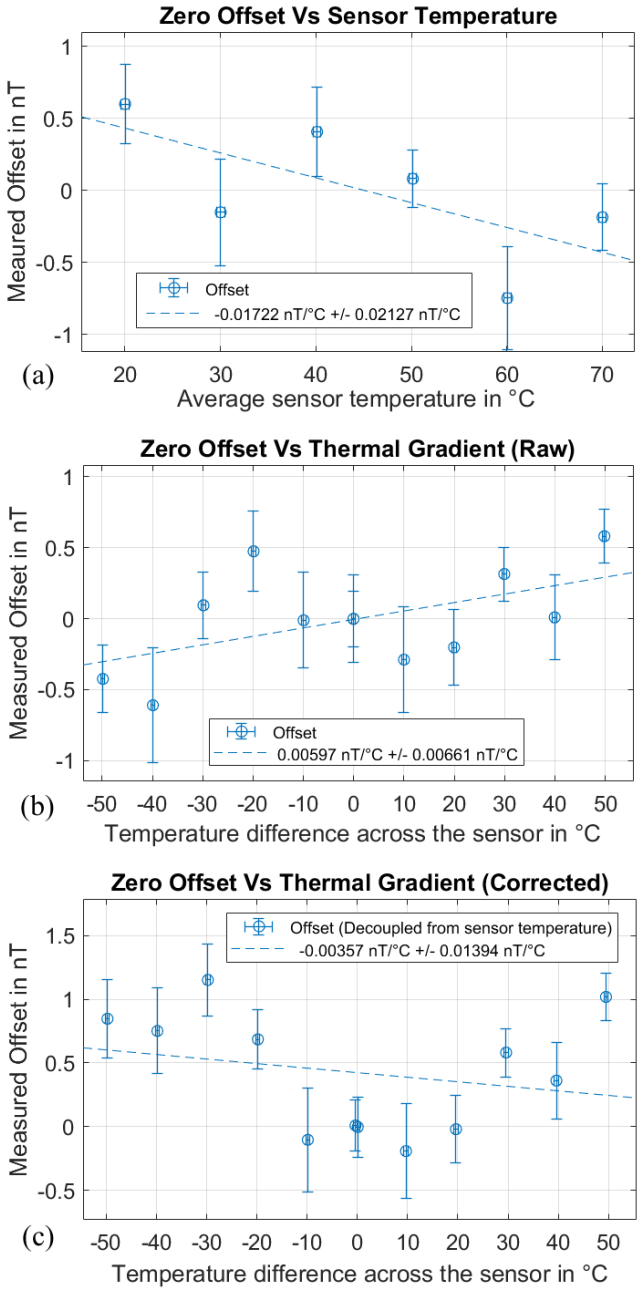

Figure 6 (a) The measured changes in offset at each temperature from 20 degrees to 70 degrees in intervals of 10 degrees. (b) The fluxgate offset when both the thermal gradient and average sensor temperature change. (c) The fluxgate offset over changes in thermal gradient decoupled from average sensor temperature. The offset does not have a strong trend with either average temperature or thermal gradient.

Figure 6a shows the measured offset plotted against the average temperature of the core. There may be a very slight downward trend (-0.017 nT/°C +/- 0.021 nT/°C) of offset with increasing temperature (Figure 6a). Changes in fluxgate sensor temperature has been known to correlate with offset drifts (i.e, Ripka 2003; Nishio et al., 2007). However, when thermal gradients as large as +/- 50 °C were applied across the sensor we did not observe statisically significant trends in offset to within +/- 0.695 nT (Figure 6c).

3.3 Instrumental Noise Floor

The instrumental noise floor of fluxgates has been known to decrease with increasing temperature (Scouten 1972; Butta et al., 2015; Rühmer et al., 2015), presumably as the permalloy gets closer to its Currie temperature. It has been suggested that thermal gradients across the fluxgate core could be one of the causes of increase in instrumental noise (Petrucha and Kasper 2010) due to differences in strain applied on the magnetic permalloy core.

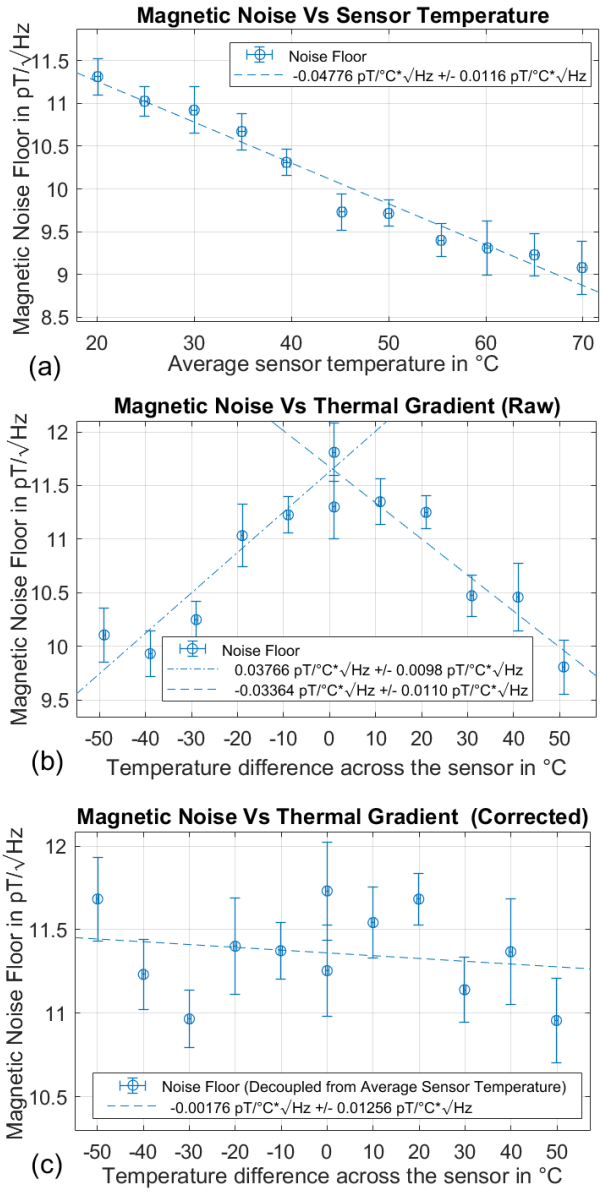

Figure 7. (a) The instrumental noise floor at 1 Hz is estimated for each temperature from 20 C to 70 C in intervals of 5 degrees. The noise is found to decrease with average sensor temperature. (b) The instrumental noise at 1 Hz is plotted against thermal gradient imposed across the core. (c) The magnetic noise over changes in thermal gradient when the change in average core temperature is accounted for. Noise was not observed to have a relationship to thermal gradient that is independent of average sensor temperature.

To characterize the effects of thermal gradients on the racetrack core's noise floor over a range of temperatures and thermal gradients, the instrumental noise floor at 1 Hz was characterized using the same method detailed in Miles et al., 2022. The solenoid was powered off and 15 minutes of quiet data was taken with the core and sensor inside the magnetic shield for each temperature step and configuration shown in Figure 3. Welch's method of overlapped periodograms (Welch 1967) was used to estimate the power spectral density noise floor for the data at temperature and thermal gradient shown in Figure 2.

Then a robust linear regression was used to fit a linear trend to the noise floor from 0.05 to 1.0 Hz. The value of this fit at 1 Hz provides a quantitative estimate of the intrinsic magnetic noise of the core at 1 Hz for every temperature step in Figure 2. The uncertainties of this linear fit are plotted as error bars. We find that this estimate of the instrumental noise floor decreases -0.0477 pT/√ Hz°C which is consistent with previous literature (Scouten 1972; Butta et al., 2015; Rühmer et al., 2015). However, the instrumental noise estimate was not found to change to within +/- 1.26 pT/√ Hz independently from average sensor temperature when thermal gradients are applied in the range of -50 °C to 50 °C.

4 Conclusions

We observe robust dependence of sensitivity and magnetic noise on sensor temperature that is consistent with existing literature. We observe similar trends when an extremely large thermal gradient is applied across the sensor. However, the effect is completely removed when the data is corrected for the average sensor temperature. Therefore, we do not observe a change in sensitivity over thermal gradient that cannot be described by the change in average scalar sensor temperature to within +/- 0.131 nT RMS. We find that gradients across the racetrack sensor bobbin have no effect on sensitivity to within +/- 26.2 ppm per degree Celsius imposed across the sensor. We do not observe changes in offset that correlate with thermal gradient independent of scalar temperature to within +/- 0.695 nT. Changes in instrumental noise floor over thermal gradient is also not observed to be greater than +/- 1.26 pT/√ Hz. Hysteresis loops over temperature or thermal gradient are not observed for sensitivity, offset, or noise (data with temperature increasing is nearly identical to data when temperature is decreasing).

It is important to note that the instrument tested in this study is different than those on the missions described above in a few important ways. In this paper, we only explore a single axis fluxgate without magnetic feedback. In these three axis sensors, these changes could be due to changes in axis alignment, as observed in Adams et al., 1976, which measured changes of 0.2 arcseconds per degrees gradient across the sensor. In these tests, we investigate only sensitivity, offset, and noise when temperature and temperature differences are static. It is possible that these changes in fluxgate calibration are due to sudden temporal differences in temperature or 'thermal shocks' rather than spatially different thermal gradients such as those observed by the Swarm magnetometers (Tøffner-Caulsen et al., 2016).

The thermal gradients imposed across the sensor in this experiment are roughly an order of magnitude greater than those observed on the MMS Spacecraft (Bromound et al., 2021), the GOES-16 mission (Loto'aniu et al., 2019), the CHAMP VFM (Brauer et al., 1999) and the K-2A satellite (Magnes et al., 2020). Based on these results, it may be useful to investigate these anomalous changes in on-orbit calibration in the context of other error sources, such as the

sensor temperature being slightly thermally decoupled from the actual average sensor temperature.

Acknowledgments

The authors are greatly indebted to Amanda Lasko. This work would not have been possible if it were not for her oversight and management of the prototype manufacturing and testing processes. A very special thanks to Samuel Hisel for his efforts building a beautiful 4 channel RTD circuit board that greatly simplified the testing procedure and made the authors lives much easier. A special thanks to Laura Ellen Greene for her assistance in editing. The authors would also like to thank Katherine Deasy for her work in configuration management and Aiyana G. Mennega for her assistance in proofreading.

Early development activities and much of the research infrastructure used in this work was supported by faculty start-up funding for David Miles from the University of Iowa. This material is based upon work supported by the National Aeronautics and Space Administration under Grant No. 80NSSC19K0491 issued through the Science Mission Directorate and Contract No. 80GSFC18C0008 administered by Goddard Space Flight Center

Open Research

Availability Statement:

The data described in this manuscript and the software used in its analysis can be accessed at the Harvard Dataverse Repository cited below:

Greene, K. (2023), Data and Software for: Thermal Gradient Testing on Fluxgate Sensors, Harvard Dataverse https://doi.org/10.7910/DVN/YLMHQJ

References

Acuña, M.H., Scearce, C.S., Seek, J. and Scheifele, J. (1978), The MAGSAT vector magnetometer: A precision fluxgate magnetometer for the measurement of the geomagnetic field. *NASA Technical Memorandum, 79656*

Alconcel, L.N.S., Fox, P., Brown, P., Oddy, T.M., Lucek, E.L. and Carr, C.M. (2014), An initial investigation of the long-term trends in the fluxgate magnetometer (FGM) calibration parameters on the four Cluster spacecraft. *Geoscientific Instrumentation, Methods and Data Systems*, *3*(2), pp.95-109. https://doi.org/10.5194/gi-3-95-2014

Baumjohann, W., Matsuoka, A., Narita, Y., Magnes, W., Heyner, D., Glassmeier, K.H., Nakamura, R., Fischer, D., Plaschke, F., Volwerk, M. and Zhang, T.L. (2020), The BepiColombo–Mio magnetometer en route to Mercury. *Space Science Reviews*, *216*, pp.1-33.

Brauer, P., Merayo, J. M. G., Risbo, T., and Primdahl, F. (1999), Magnetic calibration of vector magnetometers, *Workshop on Calibration of Space-Borne Magnetometers, Institute of Geophysics and Meteorology, Technical University of Braunschweig.* https://doi.org/10.1007/s11214-020-00754-y

Bromund, K., Huang, B., Anderson, B., Le, G., Wei, H., Russell, C., Plaschke, F., Fischer, D., Magnes, W., Zara, R. and Rosanova, S. (2021), December. Crucial Role of Thermal Gradients in MMS Fluxgate In-Flight Calibration. In *AGU Fall Meeting Abstracts Vol. 2021*, pp. SH35D-2103.

354 Butta M., Ripka P., Janosek M., Pribil M. (2015), Electroplated FeNi ring cores for fluxgates
355 with field induced radial anisotropy. *Journal of Applied Physics*, 117,17A722.
356 https://doi.org/10.1063/1.4914874
357
358 Connerney, J.E.P., Acuna, M.H., Wasilewski, P.J., Kletetschka, G., Ness, N.F., Reme, H., Lin,
359 R.P. and Mitchell, D.L., 2001. The global magnetic field of Mars and implications for crustal
360 evolution. *Geophysical Research Letters*, *28*(21), pp.4015-4018.
361 https://doi.org/10.1029/2001GL013619
362
363 Ferreira, N. J., Antunes, P. J., Viana, J. C., Fernandes, L. C., Fernandez, E., and Lanceros-
364 Mendez, S. (2019), Magnetic Field Perturbations by Thermoelectric Effects. *2019 ESA*
365 *Workshop on Aerospace EMC*, Budapest, Hungary, 1–6,
366 https://doi.org/10.23919/AeroEMC.2019.8788964
367
368 Gjerloev, J.W., Ohtani, S., Iijima, T., Anderson, B., Slavin, J. and Le, G. (2011), October.
369 Characteristics of the terrestrial field-aligned current system. In *Annales Geophysicae* (Vol. 29,
370 No. 10, pp. 1713-1729). Göttingen, Germany: Copernicus
371 Publications.https://doi.org/10.5194/angeo-29-1713-2011
372
373 Greene, K., Hansen, C., Narod, B. B., Dvorsky, R., and Miles, D. M. (2022), Tesseract – a high-
374 stability, low-noise fluxgate sensor designed for constellation applications. *Geosci. Instrum.*
375 *Method. Data Syst*., 11, 307–321, https://doi.org/10.5194/gi-11-307-2022
376

Greene, K. (2023), Data and Software for: Thermal Gradient Testing on Fluxgate Sensors, *Harvard Dataverse* https://doi.org/10.7910/DVN/YLMHQJ,

Hou D., Qui Z., Iguchi R., Sato K., Vehstedt E. K., Uchida K., Bauer G. E., Saitoh E. (2016), Observation of temperature-gradient-induced magnetization, Nature Communications, 12265, https://doi.org/10.1038/ncomms12265

Jager, T., Leger, J. M., Fratter, I., Lier, P., and Pacholczyk, P. (2016), Magnetic cleanliness and thermomagnetic effect: Case study of the absolute scalar magnetometer and its environment on swarm satellites, in: 2016 ESA Workshop on Aerospace EMC (Aerospace EMC), Valencia, Spain, 1–6, https://doi.org/10.1109/AeroEMC.2016.7504584

Jain, S., Lam, D. D., Bose, A., Sharma, H., Palkar, V. R., Tomy, C. V., Suzuki, Y., and Tulapurkar, A. A. (2014), Magneto-Seebeck effect in spin-valve with in-plane thermal gradient, *AIP Advances*, 4, 127145, https://doi.org/10.1063/1.4905137

Loto'aniu, T.M., Redmon, R.J., Califf, S., Singer, H.J., Rowland, W., Macintyre, S., Chastain, C., Dence, R., Bailey, R., Shoemaker, E. and Rich, F.J. (2019), The GOES-16 spacecraft science magnetometer. *Space Science Reviews*. *215*, 1-28. https://doi.org/10.1007/s11214-019-0600-3

Lühr, H., Yin, F., and Bock, R. (2013), Magnetic properties of CHAMP and their effects on in-orbit calibration. *J. Sens. Sens. Syst*, 2, 9–17, https://doi.org/10.5194/jsss-2-9-2013

Lühr, H., Park, J., Gjerloev, J.W., Rauberg, J., Michaelis, I., Merayo, J.M. and Brauer, P., 2015. Field-aligned currents' scale analysis performed with the Swarm constellation. *Geophysical Research Letters*, *42*(1), pp.1-8. https://doi.org/10.1002/2014GL062453

Magnes, W., Hillenmaier, O., Auster, H. U., Brown, P., Kraft, S., Seon, J., M. Delva, A. Valavanoglou, S. Leitner1, D. Fischer, G. Berghofer1, Y. Narita, F. Plaschke, M. Volwerk, J. Wilfinger, C. Strauch, J. Ludwig, D. Constantinescu, K. H. Fornacon, K. Gebauer, D. Hercik, I. Richter, J.P. Eastwood, J.P. Luntama, A. Hilgers, M. Heil, G.W. Na, Lee, C. H. (2020), Space weather magnetometer aboard GEO-KOMPSAT-2A. *Space Science Reviews*, *216*, 1-36. https://doi.org/10.1007/s11214-020-00742-2

McNeil, W.J. (1993), Aspects of the Calibration and Processing of the CRRES Fluxgate Magnetometer Data. *RADEX INC BEDFORD MA*.

Miles, D. M., Mann, I. R., Kale, A., Milling, D. K., Narod, B. B., Bennest, J. R., Barona, D., and Unsworth, M. J. (2017), The effect of winding and core support material on the thermal gain dependence of a fluxgate magnetometer sensor, *Geosci. Instrum. Method. Data Syst*., 6, 377–396, https://doi.org/10.5194/gi-6- 377-2017

Miles, D. M., Ciurzynski, M., Barona, D., Narod, B. B., Bennest, J. R., Kale, A., Lessard, M., Milling, D. K., Larson, J., and Mann, I. R. (2019), Low-noise permalloy ring cores for fluxgate magnetometers. *Geosci. Instrum. Method. Data Syst.*, 8, 227–240, https://doi.org/10.5194/gi-8-227-2019

Miles, D. M., Howarth, A. D., & Enno, G. A. (2019), In situ calibration of offsetting magnetometer feedback transients on the Cassiope spacecraft. *Geoscientific Instrumentation, Methods and Data Systems*, *8*(2), 187-195. https://doi.org/10.5194/gi-8-187-2019.

Miles, D. M., Dvorsky, R., Greene, K., Hansen, C. T., Narod, B. B., and Webb, M. D. (2022), Contributors to fluxgate magnetic noise in permalloy foils including a potential new copper alloy regime. *Geosci. Instrum. Method. Data Syst*, 11, 111–126, https://doi.org/10.5194/gi-11-111-2022

Nishio Y, Tohyama F, Onishi N. (2007), The sensor temperature characteristics of a fluxgate magnetometer by a wide-range temperature test for a Mercury exploration satellite. *Measurement Science and Technology*, 18(8):2721. https://doi.org/10.1088/0957-0233/18/8/050

Olsen, N., Ravat, D., Finlay, C.C. and Kother, L.K. (2017), LCS-1: a high-resolution global model of the lithospheric magnetic field derived from CHAMP and Swarm satellite observations. *Geophysical Journal International*, *211*(3), pp.1461-1477. https://doi.org/10.1093/gji/ggx381

Olsen, N. (2021), Magnetometer data from the GRACE satellite duo, *Earth Planets Space*, 73, 62, https://doi.org/10.1186/s40623-021-01373-9

445 Petrucha, V. and Kaspar, P. (2010), Compact fluxgate sensor with a vector compensation of a
446 measured magnetic field, in: *2010 IEEE Sensors, 2010 Ninth IEEE Sensors Conference*, Kona,
447 HI, 1795–1798, https://doi.org/10.1109/ICSENS.2010.5689982,
448
449 Primdahl, F. (1979), The fluxgate magnetometer. J. Phys. E: Sci. Instrum., 12, 241–
450 253, https://doi.org/10.1088/0022-3735/12/4/001
451
452 Qiu, Y., Wang, Z., Jiang, W., Zhang, B., Li, F. and Guo, F., 2017. Combining CHAMP and
453 Swarm satellite data to invert the lithospheric magnetic field in the Tibetan
454 Plateau. *Sensors*, *17*(2), p.238. https://doi.org/10.3390/s17020238
455
456 Ripka, P. (2003), Advances in fluxgate sensors. *Sensors and Actuators A: Physical*, 106, 8–
457 14, https://doi.org/10.1016/S0924-4247(03)00094-3
458
459 Ripka, P. (2008), Sensors based on bulk soft magnetic materials: Advances and
460 challenges. *Journal of Magnetism and Magnetic Materials*, *320*(20), pp.2466-2473.
461 https://doi.org/10.1016/j.jmmm.2008.04.079
462
463 Rühmer, D., Bögeholz, S., Ludwig, F., and Schilling, M. (2015), Vector fluxgate magnetometer
464 for high operation temperatures up to 250°C. *Sensors and Actuators A: Physical*, 228, 118–124,
465 https://doi.org/10.1016/j.sna.2015.03.004
466

Sebbes, P., Ludwig, F. and Schilling, M. (2010), Fluxgate magnetometer for temperatures up to 180 C. *J. Electr. Eng*, *61*, 21-3.

Scouten D. (1972), Sensor noise in low-level flux-gate magnetometers. *IEEE Transactions on Magnetics*. 8(2), 223-31. 10.1109/TMAG.1972.1067284

Trigg, D. F., Serson, P. H., and Camfield, P. A. (1971), A solid-state electrical recording magnetometer, vol. 41, *Publ. Earth Phys. Branch, Dept. Energy, Mines and Resources*. 66–80.

Tøffner-Clausen, L., Lesur, V., Olsen, N., and Finlay, C. C. (2016), In-flight scalar calibration and characterization of the Swarm magnetometry package, *Earth Planet Sp*, 68, 129, https://doi.org/10.1186/s40623-016-0501-6

Welch P. (1967), The use of fast Fourier transform for the estimation of power spectra: a method based on time averaging over short, modified periodograms, *IEEE Transactions on audio and electroacoustics*, 7, 70-73, https://doi.org/0.1109/TAU.1967.1161901